

## Original Paper

# Mechanisms Underlying H<sub>2</sub>O<sub>2</sub>-Evoked Carbonyl Modification of Cytoskeletal Protein and Axon Injury in PC-12 Cells

Xiejun Zhang<sup>a,b</sup> Zongyang Li<sup>b,c</sup> Qiusheng Zhang<sup>a,b</sup> Lei Chen<sup>a,b</sup>  
Xianjian Huang<sup>a,b</sup> Yuan Zhang<sup>b,c</sup> Xiaojia Liu<sup>a</sup> Wenlan Liu<sup>b,c</sup> Weiping Li<sup>a,b</sup>

<sup>a</sup>Department of Neurosurgery, Shenzhen University First Affiliated Hospital, Shenzhen Second People's Hospital, Clinical College of Anhui Medical University, Shenzhen, <sup>b</sup>Shenzhen Key Laboratory of Neurosurgery, Shenzhen, <sup>c</sup>The Central Laboratory, Shenzhen University First Affiliated Hospital, Shenzhen Second People's Hospital, Clinical College of Anhui Medical University, Shenzhen, China

## Key Words

Traumatic brain injury • Oxidative stress • Cytoskeletal protein • Carbonylation • Axonal injury • Proteasome β5 subunit

## Abstract

**Background/Aims:** To investigate the mechanism that enables oxidative stress and cytoskeleton protein carbonylation to contribute to axonal dysfunction in traumatic brain injury (TBI). **Methods:** We created an *in vitro* model of neuronal oxidative damage by exposing a neuron-like cell line (PC-12) to different concentrations (100 μM, 200 μM, and 300 μM) of H<sub>2</sub>O<sub>2</sub> for 24 h or 48 h. Carbonyl modification of cytoskeletal proteins (β-actin and β-tubulin) and its impact on β-actin/β-tubulin filament dynamics were determined by enzyme-linked immunosorbent assay, immunostaining, and western blotting. Depolymerization of β-actin/β-tubulin filaments was evaluated using the monomer/polymer ratio of each protein via western blotting. Phosphorylation of the neurofilament heavy chain (P-NFH) was used as an axonal injury marker and detected by immunostaining. **Results:** Our results showed that H<sub>2</sub>O<sub>2</sub> treatment led to increased oxidative stress in PC-12 cells, as indicated by the increased generation of malondialdehyde and 8-hydroxydeoxyguanosine and decreased intracellular glutathione levels. H<sub>2</sub>O<sub>2</sub> treatment also increased carbonyl modification of total proteins and cytoskeleton proteins β-actin/β-tubulin, which occurred concurrently with the suppression of proteasome activity. Moreover, H<sub>2</sub>O<sub>2</sub> treatment increased the generation of the axonal injury marker P-NFH, and depolymerization of the β-actin/β-tubulin filaments was indicated by increased monomer/polymer ratios of each protein. Lastly, overexpression of the proteasome β5 subunit in PC-12 cells significantly reduced the H<sub>2</sub>O<sub>2</sub>-induced accumulation of carbonylated β-actin/β-tubulin, P-NFH, and β-actin/β-tubulin depolymerization. **Conclusions:** We concluded that

X. Zhang, Z. Li and Q. Zhang contributed equally to the work

Weiping Li, MD & PhD  
and Wenlan Liu, MD & PhD

Dept. of Neurosurgery, Shenzhen Key Lab. of Neurosurgery, Shenzhen Univ. first Aff. Hosp.  
Shenzhen Second People's Hospital, Shenzhen 518035 (China)  
Tel. 86-755-83366388, Fax 86-755-83676000, E-Mail wpli@szu.edu.cn, wliu@szu.edu.cn

carbonylation of cytoskeleton proteins could lead to depolymerization of their filaments and axonal injury, and proteasome suppression contributes to the accumulation of carbonylated proteins under oxidative conditions.

© 2018 The Author(s)  
Published by S. Karger AG, Basel

## Introduction

Traumatic brain injury (TBI) results from an impact to the head that disrupts normal brain function. Severe TBI can cause permanent brain damage or death [1]. Diffuse axonal injury (DAI) is a typical pathological change after TBI and is closely associated with clinical prognosis [2]. DAI has two distinct pathological features: swellings and large terminal bulbs due to excessive neurofilament aggregation [3, 4]. Secondary axonal injury resulting from cytoskeleton abnormalities is the most common cause of DAI [5, 6].

Oxidative stress is a well-known factor implicated in DAI [7], and the mitochondrial phosphorylating capacity, concentrations of the nicotinic coenzyme pool, and oxidative/nitrosative stress correlate closely with the severity of DAI [8, 9]. Carbonyl modification occurs as a direct result of oxidative damage to proteins, leading to protein dysfunction and the formation of protein aggregates [10]. Protein carbonylation has been shown to contribute to the pathogenesis of several neurodegenerative diseases such as multiple sclerosis, Parkinson's disease, and Alzheimer's disease [11]. Under normal conditions, carbonylated proteins are thought to be degraded by proteasomes whose main function is to recognize and degrade unneeded, damaged, or misfolded proteins [12-14]. Under prooxidative conditions, however, the increased generation of reactive oxygen species (ROS) or reactive carbonyl species may reduce the activity of proteasomes [11, 15, 16], leading to the accumulation of carbonylated proteins in affected cells.

Axoplasmic transport, also called axonal transport, is a cellular process responsible for the movement of mitochondria, lipids, synaptic vesicles, proteins, and other cell parts (i.e., organelles) to and from the neuron cell body through the cytoplasm of the axon [17]. Normal axonal transport depends on normal formation of the cytoskeletal structure of neurons. Under TBI conditions, cytoskeleton proteins—in particular actin—could be carbonylated due to excessive ROS generation in affected neurons [11, 18-20]. However, whether cytoskeleton protein carbonylation contributes to axonal dysfunction in TBI remains unknown.

In the present study, we generated an *in vitro* model of neuronal oxidative damage by exposing a neuron-like cell line (PC-12) to H<sub>2</sub>O<sub>2</sub> to investigate carbonyl modification of cytoskeletal proteins ( $\beta$ -actin and  $\beta$ -tubulin) and the impact on  $\beta$ -actin/ $\beta$ -tubulin filament dynamics. Our data show that H<sub>2</sub>O<sub>2</sub> exposure increased  $\beta$ -actin/ $\beta$ -tubulin carbonylation, which promoted the depolymerization of these proteins and the generation of an axonal injury marker, namely, the phosphorylation of neurofilament heavy chain (P-NFH). Moreover, all these changes were significantly reversed by proteasome  $\beta$ 5 subunit overexpression.

## Materials and Methods

### Materials

PC-12 cells were obtained from the Cell Resource Center of the Institute of Basic Medical Sciences, Peking Union Medical College/Chinese Academy of Medical Sciences (Beijing, China). Dulbecco's modified Eagle's medium (DMEM), fetal bovine serum (FBS), horse serum, and Lipofectamine 2000 were purchased from Life Technologies (Grand Island, NY, USA). H<sub>2</sub>O<sub>2</sub>, penicillin, and streptomycin were purchased from Sigma-Aldrich (St. Louis, MO, USA). Malondialdehyde (MDA) and glutathione (GSH) detection kits were purchased from the Nanjing Jiancheng Bioengineering Institute (Nanjing, China). The primary antibodies against  $\beta$ -actin,  $\beta$ -tubulin, DNP, or neurofilaments and their corresponding secondary antibodies were purchased from Santa Cruz Biotechnology (Santa Cruz, CA, USA).

### *Cell culture and treatments*

The neuron-like PC-12 cells were grown on DMEM supplemented with 10% (v/v) heat-inactivated fetal bovine serum, 5% (v/v) heat-inactivated horse serum, 100 U/mL penicillin, and 100 µg/mL streptomycin and maintained at 37 °C in a humidified incubator ventilated with 95% air and 5% CO<sub>2</sub>. Cells in the exponential phase of growth were used in the experiments. PC-12 cells were transfected with the β5 expression vector plasmid using Lipofectamine 2000 (Life Technologies) and stable transfectants were selected in 1 mg/mL Geneticin (G418; Thermo Fisher Scientific, Waltham, MA, USA). Stable clones were maintained in DMEM supplemented with 200 µg/mL G418, 10% (v/v) heat-inactivated fetal bovine serum, 5% (v/v) heat-inactivated horse serum, 100 U/mL penicillin, and 100 µg/mL streptomycin. Cells were treated with different concentrations (100 µM, 200 µM, and 300 µM) of H<sub>2</sub>O<sub>2</sub> for 24 h or 48 h. Cell viability was tested with CCK-8 to monitor the cytotoxicity of the H<sub>2</sub>O<sub>2</sub> concentrations.

### *Measurements of MDA, GSH, and 8-hydroxydeoxyguanosine (8-OHdG)*

PC-12 cells at ~90% confluence in six-well plates were subjected to the indicated H<sub>2</sub>O<sub>2</sub> treatments before measuring the biomarkers (MDA, GSH, & 8-OHdG) for oxidative stress using commercial assay kits.

MDA assay was performed using an Abcam kit (Catalog No. ab118970; Cambridge, UK). In brief, the cells were lysed in MDA lysis solution. After centrifugation at 13,000 g for 10 min, supernatants were collected, and the total protein concentration was determined by a bicinchoninic acid assay. The supernatant was mixed with thiobarbituric acid (TBA) solution and incubated at 95 °C for 60 min. The MDA-TBA adduct was determined by absorbance at 532 nm. A calibration curve was obtained using MDA standard solution, and each curve point was subjected to the same treatment as that of the supernatants. TBA-MDA content was calculated as nanomoles of MDA formed per milligram of protein and expressed as the percentage of the value for untreated control cells.

GSH was assessed with a kit from Cayman Chemical Co. (Item No. 703002; Ann Arbor, MI, USA). In brief, the cells were harvested using a rubber policeman and homogenized in cold MES buffer containing 1 mM EDTA. After centrifugation at 10,000 g for 15 min, supernatants were collected and mixed with equal volumes of metaphosphoric acid solution. After centrifugation at 3000 g for 3 min, the resultant supernatants were mixed with triethanolamine at a ratio of 20:1 (vol/vol) and then incubated with freshly prepared Assay Cocktail for 25 min. After incubation, the absorbance of each sample was read at 410 nm. A calibration curve was obtained using oxidized glutathione (GSSG) standard. Total GSH content was calculated as nanomoles of GSSG formed per milligram of protein. Quantification of GSSG, exclusive of GSH, was accomplished by derivatizing GSH with 2-vinylpyridine before incubation with the Assay Cocktail. The amount of reduced GSH was calculated by subtracting GSSG from total GSH and it was expressed as percentage of the value untreated control cells.

The amount of 8-OHdG was measured using an enzyme-linked immunosorbent assay kit from Cell Biolabs Inc. (Catalog No. STA-320; San Diego, CA, USA). In brief, at the end of treatment, DNA was extracted from PC-12 cells and denatured at 95 °C for 5 min. After digestion, the sample was added to an 8-OHdG conjugate-coated plate and absorbance was read at 450 nm. A calibration curve was obtained using 8-OHdG standard. The content of 8-OHdG was calculated as nanograms per milligram of DNA and expressed as a percentage of the value for untreated control cells.

### *Measurement of protein carbonyls*

Carbonyl content was assessed using a protein carbonyl content assay kit (Abcam, ab126287) according to the manufacturer's instructions. This assay was based on the reaction of protein carbonyls with dinitrophenylhydrazine (DNPH) to form dinitrophenylhydrazone, a yellow compound, measured spectrophotometrically at 375 nm. Briefly, after H<sub>2</sub>O<sub>2</sub> treatment, the cells were harvested and homogenized in lysis buffer. After centrifugation, protein concentrations of cell lysates were quantified using a BCA Protein Assay (Abcam, ab102536). Lysates (100 µL) were added to plastic tubes containing 100 µL DNPH solution. Samples were vortexed and incubated for 15 min at room temperature. Subsequently, trichloroacetic acid solution (30 µL) was added to each tube. The mixture was vortexed and centrifuged at 14,000 × g for 2 min and the supernatant obtained was discarded. The pellet was washed with 0.5 mL acetone, sonicated for 30 s, and placed at -20 °C for 5 min. After centrifugation at 14,000 × g for 2 min, the supernatant was discarded, and the pellet was re-suspended in 200 µL of guanidine solution and sonicated briefly. Samples were then

centrifuged at  $14,000 \times g$  for 2 min, 100  $\mu$ L of the supernatant was transferred to a 96-well plate, and the absorbance at was measured at 375 nm. Results were recorded as percentage of the value for untreated control cells.

### *Measurement of proteasome activity*

Proteasome activity was assessed using Amplitude™ Fluorometric Proteasome 20S Assay Kit (CNHAOBIO, Beijing, China) according to manufacturer's instructions. In brief, PC-12 cells grown in a 96-well plate underwent the treatments before incubation with a proteasome assay loading solution at 37 °C for 2 h. Fluorescence intensity was measured at an excitation wavelength of 490 nm and emission wavelength of 525 nm. Results were reported as relative fluorescence unit (RFU).

### *Immunostaining*

PC-12 cells were seeded on poly-L-lysine-coated coverslips and fixed by incubation with 4% paraformaldehyde in PBS for 10 min at room temperature. Cells were permeabilized with 0.1% Triton-X 100 for 10 min and then blocked with 1 % BSA for 1 h. Cells were rinsed with PBS and incubated with antibodies against  $\beta$ -actin (dilution, 1:500),  $\beta$ -tubulin (dilution, 1:500), DNP (dilution, 1:500) or P-NFH (dilution, 1:500) overnight at 4 °C, followed by incubation with Alexa Fluor® 488-conjugated goat anti-rabbit (dilution, 1:500) or Alexa Fluor® 594-conjugated goat anti-mouse secondary antibodies (dilution, 1:500) for 30 min at room temperature in the dark. After washing with PBS, the coverslips were incubated in PBS containing DAPI for 15 min and visualized under a fluorescence microscope (Leica Camera AG, Wetzlar, Germany). Cells incubated in the absence of primary antibodies served as negative controls and were not immunoreactive (data not shown).

### *Western blot*

After the treatments, PC-12 cells were harvested and lysed with RIPA lysis buffer supplemented with protease inhibitor cocktail (Roche, Indianapolis, IN, USA). Whole cell lysates were centrifuged at 12,000 g for 15 min at 4 °C, and the supernatants were collected. Total protein concentration was determined by the bicinchoninic acid assay. Protein samples (30  $\mu$ g protein/lane) were separated by electrophoresis on 10% sodium dodecyl sulfate polyacrylamide gels before transferring onto nitrocellulose membranes. The membranes were incubated with 5% (w/v) non-fat milk in Tris-buffered saline containing 0.1% (v/v) Tween-20 for 2 h to block nonspecific binding, incubated overnight at 4 °C with primary antibodies against  $\beta$ -actin or  $\beta$ -tubulin, and then incubated with the corresponding HRP-conjugated goat anti-mouse or goat anti-rabbit secondary antibodies. The membranes were developed with Amersham ECL western blotting detection reagents (GE Healthcare, Chicago, IL, USA) and photographed via a BioSpectrum Imaging System (Thermo Fisher Scientific).

### *Statistical analysis*

All data were expressed as means  $\pm$  SD. Differences between groups were evaluated by one-way ANOVA followed by Newman-Keuls multiple comparisons test.  $P < 0.05$  was considered statistically significant.

## Results

### *Protein carbonylation and proteasome inhibition in H<sub>2</sub>O<sub>2</sub>-treated PC-12 cells*

To assess carbonyl modification of proteins under oxidative stress, we first established an *in vitro* oxidative stress model by exposing PC-12 cells to various concentrations of H<sub>2</sub>O<sub>2</sub> for up to 48 h. Three biomarkers for oxidative stress were analyzed to validate this model. As shown in Fig. 1, following H<sub>2</sub>O<sub>2</sub> treatment, the level of intracellular GSH (reduced form) was significantly reduced, and accordingly, the amounts of MDA and 8-OHdG were significantly increased. Moreover, these changes were dose- and time-dependent (Fig. 1A–F).

We then assessed protein carbonylation in H<sub>2</sub>O<sub>2</sub>-treated PC-12 cells by measuring carbonyls using a DNPH tagging method. H<sub>2</sub>O<sub>2</sub> treatment increased the amounts of protein carbonyls in a dose- and time-dependent manner (Fig. 2A & B).

**Fig. 1.** H<sub>2</sub>O<sub>2</sub> treatment induced oxidative stress in PC-12 cells. PC-12 cells were incubated with 0 μM, 100 μM, 200 μM, or 300 μM of H<sub>2</sub>O<sub>2</sub> for 24 or 48 h before GSH, MDA and 8-OHdG levels were measured. H<sub>2</sub>O<sub>2</sub> treatment significantly reduced intracellular GSH levels (A and B) and increased the amounts of MDA (C and D) and 8-OHdG (E and F) in a time- and dose-dependent manner. For the experiments in B, D, and F, the cells were treated with 200 μM H<sub>2</sub>O<sub>2</sub>. Data are expressed as means ± SD; n = 3; \*P<0.05.

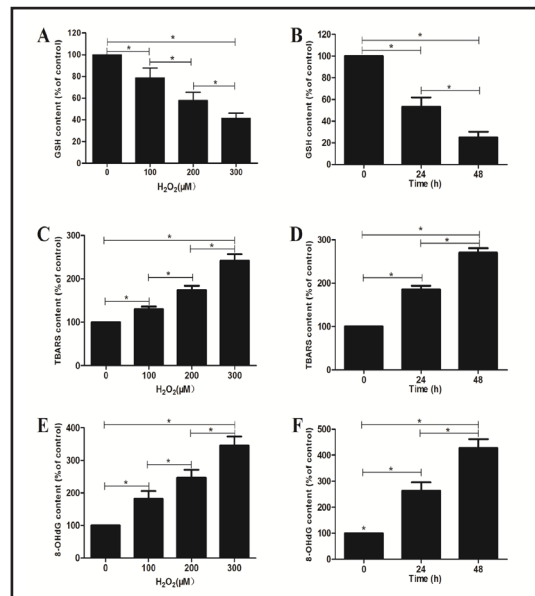
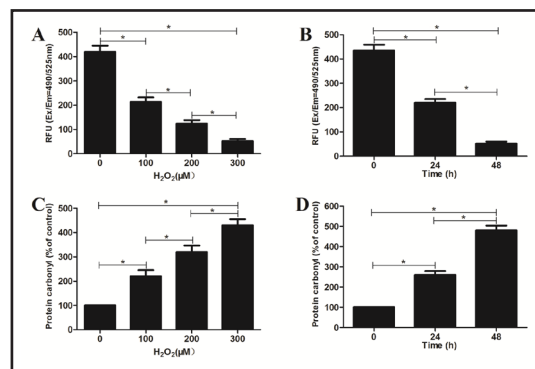


**Fig. 2.** The effects of H<sub>2</sub>O<sub>2</sub> on proteasome activity and protein carbonylation in PC-12 cells. PC-12 cells were incubated with 0 μM, 100 μM, 200 μM, or 300 μM of H<sub>2</sub>O<sub>2</sub> for 24 h or 48 h before proteasome activity and protein carbonylation were assessed. H<sub>2</sub>O<sub>2</sub> treatment suppressed proteasome activity (A and B) and increased protein carbonylation (C and D) in PC-12 cells in a time- and dose-dependent manner. For experiments B and D, the cells were treated with 200 μM H<sub>2</sub>O<sub>2</sub>. Data are expressed as means ± SD; n = 3; \*P<0.05.

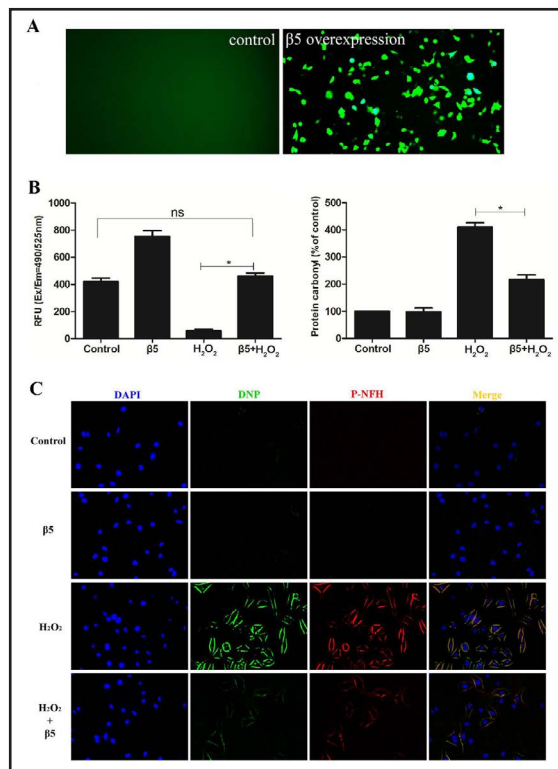


The proteasome degradation pathway is responsible for the breakdown of carbonylated proteins; therefore, we assessed proteasome activity in H<sub>2</sub>O<sub>2</sub>-treated PC-12 cells by measuring the cleavage of the fluorogenic indicator LLVY-R110. H<sub>2</sub>O<sub>2</sub> treatment led to a significant reduction in the generation of fluorescent R110, and this reduction was dose- and time-dependent, indicating suppressed proteasome activity in the cells (Fig. 2C & D). For the tested concentrations of H<sub>2</sub>O<sub>2</sub>, CCK-8 assay revealed cytotoxicity (~20% cell death) at 300 μM, while no significant cytotoxicity was observed at the other two doses (data not shown). Therefore, in subsequent experiments, we chose 200 μM H<sub>2</sub>O<sub>2</sub> as the oxidative stimulus.

#### *Overexpression of proteasome β5 inhibited H<sub>2</sub>O<sub>2</sub>-induced protein carbonylation in PC-12 cells*

To establish a causal link between the suppression of proteasome activity and the accumulation of carbonylated proteins in H<sub>2</sub>O<sub>2</sub>-challenged PC-12 cells, PC-12 cells overexpressing the proteasome β5 subunit were exposed to 200 μM H<sub>2</sub>O<sub>2</sub> for 24 h. Fig. 3A shows that cells transfected with the β5 subunit expression vector displayed strong green fluorescence, which indicates overexpression of the proteasome β5 subunit, while no fluorescence was observed in cells transfected with the control vector. Moreover, proteasome β5 subunit overexpression led to a significant increase in proteasome activity, which was partially inhibited by H<sub>2</sub>O<sub>2</sub> treatment (Fig. 3B). Of note, overexpression of the proteasome β5 subunit significantly inhibited H<sub>2</sub>O<sub>2</sub>-induced protein carbonylation in PC-12 cells (Fig. 3B, right panel). Similar results were obtained by immunostaining, in which DNP tagging was used to label carbonyl groups (Fig. 3C).

**Fig. 3.** Overexpression of proteasome  $\beta 5$  inhibits  $H_2O_2$ -induced protein carbonylation and NFH phosphorylation in PC-12 cells. PC-12 cells were transfected with proteasome  $\beta 5$  overexpressing vector or the control vector before they were exposed to  $200 \mu M H_2O_2$ . Protein carbonylation and NFH phosphorylation were detected 24 h after  $H_2O_2$  treatment. A. Fluorescence micrographs showed proteasome  $\beta 5$  subunit expression (green fluorescence) after transfection with the control vector (left) and  $\beta 5$  overexpressing vector (right). Magnification  $\times 200$ . B. Proteasome  $\beta 5$  overexpression significantly increased proteasome activity in PC-12 cells (left panel), which led to a significant reduction in  $H_2O_2$ -induced protein carbonylation (right panel). Data are expressed as means  $\pm$  SD;  $n = 3$ ; \*  $P < 0.05$  versus control; #  $P < 0.05$  versus  $H_2O_2$ . C. Double-immunostaining revealed that protein carbonylation (DNP tagging, green fluorescence) co-localized with NFH phosphorylation (P-NFH, red fluorescence) in  $H_2O_2$ -treated PC-12 cells, and proteasome  $\beta 5$  overexpression significantly reduced DNP and P-NFH immunostaining. DAPI staining was used to reveal the nuclei (blue). Magnification  $\times 400$ .



Immunostaining experiments were repeated three times with similar results.

### Overexpression of proteasome $\beta 5$ inhibits $H_2O_2$ -induced NFH phosphorylation in PC-12 cells

Axonal injury was assessed by measuring NFH phosphorylation, a well-known biomarker for axonal damage [21, 22]. As shown in Fig. 3C, P-NFH fluorescence was barely visible in control PC-12 cells, while it was significantly increased in  $H_2O_2$ -treated cells. Of note, P-NFH immunostaining co-localized with protein carbonylation (DNP staining) in  $H_2O_2$ -treated PC-12 cells, suggesting an association between protein carbonylation and axonal injury. Overexpression of the proteasome  $\beta 5$  subunit significantly inhibited NFH phosphorylation. These results indicate that exposure of PC-12 cells to  $H_2O_2$  induced protein carbonylation and NFH phosphorylation concurrently in PC-12 cells, and proteasome overexpression effectively ameliorated these changes.

### $H_2O_2$ increases cytoskeleton protein carbonylation in PC-12 cells

In neuronal cells, cytoskeleton proteins are responsible for the vital biological functions of the axon such as maintaining its mechanical integrity and shape and facilitating axonal transport. We speculated that carbonylation also occurs in cytoskeleton proteins in  $H_2O_2$ -treated PC-12 cells, which in turn leads to axonal injury. To test this possibility, we double-stained protein carbonyls (DNP tagging) and the cytoskeleton proteins  $\beta$ -actin and  $\beta$ -tubulin after exposing PC-12-cells to  $200 \mu M H_2O_2$  for 24 h. Indeed, DNP staining (red) and  $\beta$ -actin (green) or  $\beta$ -tubulin staining (green) were colocalized, supporting our speculation that cytoskeleton protein carbonylation occurs in  $H_2O_2$ -treated PC-12-cells (Fig. 4A,B). Of note, overexpression of the proteasome  $\beta 5$  subunit significantly inhibited the  $H_2O_2$ -induced carbonylation of both cytoskeleton proteins (Fig. 4A, B). These results indicate that exposure of PC-12 cells to  $H_2O_2$  induced cytoskeleton protein carbonylation and this change could be alleviated by proteasome overexpression.

**Fig. 4.** Effects of proteasome  $\beta 5$  overexpression on  $\beta$ -actin/  $\beta$ -tubulin carbonylation in  $H_2O_2$ -treated PC-12 cells. PC-12 cells were transfected with proteasome  $\beta 5$  overexpressing vector or control vector and incubated with  $200 \mu M H_2O_2$ . Carbonyl modification of  $\beta$ -actin/  $\beta$ -tubulin was detected by double-staining DNP and  $\beta$ -actin/  $\beta$ -tubulin 24 h after  $H_2O_2$  treatment.  $H_2O_2$  treatment induced carbonyl modification (red fluorescence) of  $\beta$ -actin (A) and  $\beta$ -tubulin (B) (green fluorescence) in PC-12 cells, while DNP fluorescence in control cells was very weak or absent. Proteasome  $\beta 5$  overexpression effectively inhibited carbonyl modification of  $\beta$ -actin/  $\beta$ -tubulin proteins. DAPI staining was used to reveal the nuclei (blue). Magnification  $\times 200$ . Experiments were repeated three times with similar results.

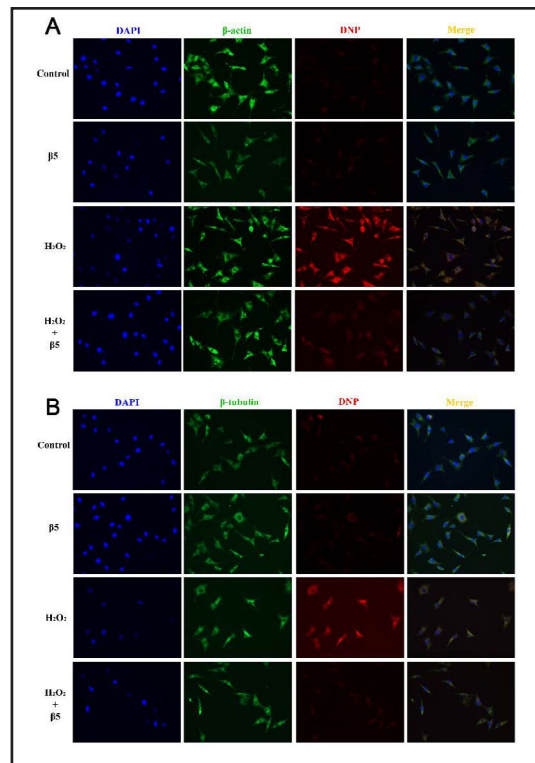
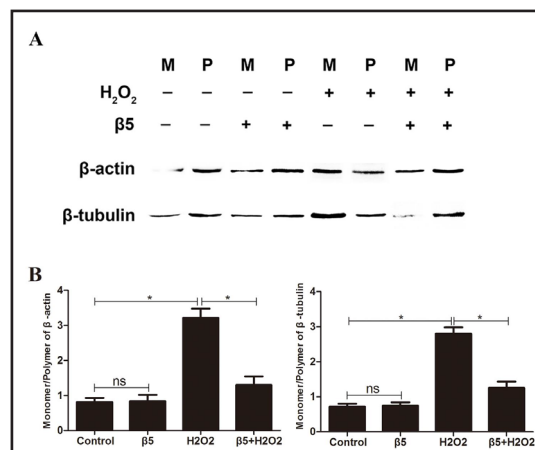


**Fig. 5.**  $H_2O_2$  treatment promotes depolymerization of  $\beta$ -actin/ $\beta$ -tubulin filaments in PC-12 cells. PC-12 cells were transfected with proteasome  $\beta 5$  overexpressing vector or control vector before incubating with  $200 \mu M H_2O_2$ .  $\beta$ -actin and  $\beta$ -tubulin filament monomers and polymers were detected by western blot 24 h after  $H_2O_2$  treatment. A. Representative western blots showing  $\beta$ -actin and  $\beta$ -tubulin filament monomer and polymer bands. B. Quantitative analyses of band intensity showed that  $H_2O_2$  treatment significantly increased the monomers/polymers ratios of  $\beta$ -actin (left panel) and  $\beta$ -tubulin (right panel) and proteasome  $\beta 5$  overexpression effectively reversed this change. Data are expressed as means  $\pm$  SD; n = 3; \* P<0.05.



#### *$\beta$ -Actin and $\beta$ -tubulin carbonylation promotes filament depolymerization*

Coordinated regulation of the polymerization and depolymerization of  $\beta$ -actin/ $\beta$ -tubulin filaments is vital for maintaining the spatially and temporally controlled dynamics of actin cytoskeletal structures within cells [23]. Our data raised the important question of whether carbonyl modification affects  $\beta$ -actin and  $\beta$ -tubulin polymerization and depolymerization. To address this question, we performed western blot analysis to detect  $\beta$ -actin/ $\beta$ -tubulin monomer and polymer levels in  $H_2O_2$ -treated PC-12 cells. As shown in Fig. 5,  $H_2O_2$  treatment significantly increased the monomer/polymer ratio of both  $\beta$ -actin and  $\beta$ -tubulin, and overexpression of the proteasome  $\beta 5$  subunit effectively reversed this change. These results indicate that carbonyl modification may disrupt the regulation of  $\beta$ -actin/ $\beta$ -tubulin polymerization and depolymerization, leading to  $\beta$ -actin/ $\beta$ -tubulin monomer accumulation in  $H_2O_2$ -treated cells, which could be partially reversed by proteasome overexpression.

## Discussion

Protein carbonylation resulting from excessive ROS generation is a common feature of TBI [11, 18, 19]; however, little is known about its significance in the pathophysiology of TBI. In this study, we investigated carbonyl modification of cytoskeletal proteins and its impact on cytoskeleton dynamics and axonal integrity in a neuron-like cell line exposed to  $H_2O_2$ . The major findings include: 1)  $H_2O_2$  treatment increased the levels of cellular oxidative markers (MDA, TABARS, 8-OHdG and protein carbonylation) and depleted intracellular GSH in PC-12 cells; 2) carbonyl modification of cytoskeleton proteins  $\beta$ -actin and  $\beta$ -tubulin occurred co-localized with NFH phosphorylation, a marker of axonal injury; 3) carbonyl modification seemed to deregulate the balance between the polymerization and depolymerization of  $\beta$ -actin/ $\beta$ -tubulin, leading to  $\beta$ -actin/ $\beta$ -tubulin monomer accumulation in  $H_2O_2$ -treated cells; 4)  $H_2O_2$  treatment suppressed proteasome activity and proteasome  $\beta 5$  subunit overexpression significantly inhibited NFH phosphorylation and  $\beta$ -actin/ $\beta$ -tubulin carbonylation and depolymerization. These results suggested that carbonyl modification of  $\beta$ -actin/ $\beta$ -tubulin disrupts cytoskeleton dynamics and causes axonal injury, and may represent an important mechanism of axonal injury following TBI.

TBI initiates a series of complex and dynamic detrimental events, such as hypoxia/ischemia, excitotoxicity, intracellular calcium overload and elevated intracranial pressure, which establish an environment of mitochondrial dysfunction to favor ROS generation [24, 25]. Thus, oxidative stress has long been implicated in the pathophysiology of TBI. As a well-documented and quantifiable indicator of oxidative stress, protein carbonylation following TBI has attracted considerable attention. Ansari et al. demonstrated the time-dependent generation of protein carbonyls in injured brain tissue following TBI, with peak values obtained at 24–48 h [26]. More recently, Lazarus et al. reported cell specificity, regional susceptibility, and gender differences in protein carbonylation after TBI [19, 27]. In a previous study, we have also shown that TBI induces oxidative stress and protein carbonylation within the injured region of the brain in a rat model of fluid percussion brain injury [28]. As a continuation of our previous study, here we have further investigated whether cytoskeleton proteins are subject to protein carbonylation in neuron-like cells exposed to oxidative stress and the effects on cytoskeletal and axonal integrity. Our data show that carbonyl modification is detected in cytoskeleton proteins  $\beta$ -actin and  $\beta$ -tubulin after  $H_2O_2$  treatment. Of note, cells with carbonyl modification of cytoskeleton proteins had increased NFH phosphorylation, which is specific to axons and considered a biomarker for axonal injury [29]. Moreover, in animal and human studies, phosphorylated NFH (p-NFH) rises significantly in both the CSF and serum, and the rise is significantly higher in more severe injuries and correlates with cortical loss [29–31]. Therefore, our data suggest that cytoskeleton protein carbonylation occurs concurrently with axonal injury in neuron-like cells exposed to oxidative stress. This observation raises two important questions. First, is there an intrinsic link between cytoskeleton protein carbonylation and NFH phosphorylation? Second, do neurofilaments, the major cytoskeleton elements in axons, also undergo carbonyl modification when neurons are exposed to oxidative stress? Future studies are warranted to examine these questions.

The axon is composed of cytoskeletal proteins, among which actin and tubulin—the two most abundant structural cytoskeletal proteins—are the cornerstones. The actin cytoskeleton plays a major role in path-finding, while the tubulin cytoskeleton provides structure to the axon shaft, serving as a scaffold. Actin and tubulin cytoskeleton interaction is fundamental for axon extension [32]. It is well known that protein carbonylation is a non-enzymatic and irreversible reaction that can destroy the structures and disrupt the functions of proteins [33]. However, in what way carbonyl modification affects the function of cytoskeleton proteins remains unknown. In our data, carbonyl modification appeared to promote both  $\beta$ -actin and  $\beta$ -tubulin to depolymerize because more filament monomers and less polymers were detected when the cells were challenged by ROS. It is known that coordinated regulation of the assembly and disassembly of actin and tubulin filaments enables spatially and temporally controlled dynamics of cytoskeletal structures within cells

[32]. Therefore, carbonyl modification of  $\beta$ -actin and  $\beta$ -tubulin may deregulate the dynamics of the cytoskeletal structures. In this study, we did not further investigate whether oxidative stress promotes the disassembly of  $\beta$ -actin and  $\beta$ -tubulin by direct carbonyl modification or by affecting their regulatory proteins, such as cyclase-associated protein, profilin, Arp2/3 activating factors, and AIP1 [34, 35].

Carbonylated proteins are thought to be degraded by the 20S proteasome [36], and degradation is ubiquitin-independent and ATP-independent [12, 13, 37]. However, under pro-oxidative conditions, the activity of the 20S proteasome appears to be inhibited via 4-hydroxy-2-nonenal (4-HNE) modification and glycation of the peptidases [38-40]. Here, our data also demonstrated that the activity of the proteasome was significantly inhibited by  $H_2O_2$  in PC-12 cells. Of note, when proteasome  $\beta 5$  subunits were overexpressed, the activities of the proteasomes in  $H_2O_2$ -treated PC12 cells were completely inhibited but comparable to the control cells, suggesting that a dose response may exist in the interaction between  $H_2O_2$  and proteasomes, and 200  $\mu M$   $H_2O_2$  may not be enough to inhibit all peptidases of the proteasome when the latter is overexpressed. In this context, the PC12 cells should still function to degrade carbonylated proteins and thus reduce oxidative damage to the axons. Indeed, our data show that overexpression of proteasome  $\beta 5$  subunits reduced  $H_2O_2$ -induced protein carbonylation, NFH phosphorylation, and depolymerization of cytoskeleton proteins, emphasizing the important role of proteasomes in the removal of carbonylated proteins and protection of the axons against oxidative injury.

Our study demonstrated that under pro-oxidant conditions, carbonyl modification of cytoskeleton proteins  $\beta$ -actin and  $\beta$ -tubulin occurred, and proteasome suppression contributed to the accumulation of carbonylated proteins in the oxidized cells. Moreover, carbonyl modification disrupted the balance between  $\beta$ -actin/  $\beta$ -tubulin polymerization and depolymerization, which could in turn lead to impaired dynamics of cytoskeletal structures and eventually axonal dysfunction of neurons in response to oxidative stress.

## Abbreviations

TBI (traumatic brain injury); DAI (diffuse axonal injury); ROS (reactive oxygen species); P-NFH (phosphorylation of neurofilament heavy chain); DMEM (Dulbecco's modified Eagle's medium); FBS (fetal bovine serum); TBA (thiobarbituric acid); MDA (malondialdehyde); GSH (glutathione); 8-OHdG (8-hydroxy-2'-deoxyguanosine); DNPH (dinitrophenylhydrazine); GSSG (oxidized glutathione); PC-12 (pheochromocytoma cell line); 4-HNE (4-hydroxy-2-nonenal); RFU (relative fluorescence unit).

## Acknowledgements

WLL, XJZ, and ZYL conceived and designed the experiments; XJZ, ZYL, QSZ and LC performed the experiments; XJZ, YZ and XJH analyzed the data; ZYL and XJL contributed reagents/materials/analysis tools; and WLL and WPL wrote the paper.

This study was supported by a grant from the National Natural Science Foundation China (Grant No. 81301062) and Shenzhen Science & Technology Commission grants (Grant Nos. ZDSYS20140509173142601, GCZX2015050411225563 and JCYJ20140414170821242).

## Disclosure Statement

The authors declare that they have no Disclosure Statement.

## References

- 1 Lu C, Xia J, Bin W, Wu Y, Liu X, Zhang Y: Advances in diagnosis, treatments, and molecular mechanistic studies of traumatic brain injury. *Biosci Trends* 2015;9:138-148.
- 2 Davceva N, Basheska N, Balazic J: Diffuse Axonal Injury-A Distinct Clinicopathological Entity in Closed Head Injuries. *Am J Forensic Med Pathol* 2015;36:127-133.
- 3 Johnson VE, Stewart W, Smith DH: Axonal pathology in traumatic brain injury. *Exp Neurol* 2013;246:35-43.
- 4 DiLeonardi AM, Huh JW, Raghupathi R: Impaired axonal transport and neurofilament compaction occur in separate populations of injured axons following diffuse brain injury in the immature rat. *Brain Res* 2009;1263:174-182.
- 5 Wang J, Hamm RJ, Povlishock JT: Traumatic axonal injury in the optic nerve: evidence for axonal swelling, disconnection, dieback, and reorganization. *J Neurotrauma* 2011;28:1185-1198.
- 6 Greer JE, Hanell A, McGinn MJ, Povlishock JT: Mild traumatic brain injury in the mouse induces axotomy primarily within the axon initial segment. *Acta Neuropathol* 2013;126:59-74.
- 7 Di Pietro V, Lazzarino G, Amorini AM, Tavazzi B, D'Urso S, Longo S, Vagnozzi R, Signoretti S, Clementi E, Giardina B, Lazzarino G, Belli A: Neuroglobin expression and oxidant/antioxidant balance after graded traumatic brain injury in the rat. *Free Radic Biol Med* 2014;69:258-264.
- 8 Tavazzi B, Signoretti S, Lazzarino G, Amorini AM, Delfini R, Cimatti M, Marmarou A, Vagnozzi R: Cerebral oxidative stress and depression of energy metabolism correlate with severity of diffuse brain injury in rats. *Neurosurgery* 2005;56:582-589.
- 9 Tavazzi B, Vagnozzi R, Signoretti S, Amorini AM, Belli A, Cimatti M, Delfini R, Di Pietro V, Finocchiaro A, Lazzarino G: Temporal window of metabolic brain vulnerability to concussions: oxidative and nitrosative stresses--part II. *Neurosurgery* 2007;61:390-395.
- 10 Rodrigo R, Libuy M, Feliu F, Hasson D: Oxidative stress-related biomarkers in essential hypertension and ischemia-reperfusion myocardial damage. *Dis Markers* 2013;35:773-790.
- 11 Zheng J, Bizzozero OA: Accumulation of protein carbonyls within cerebellar astrocytes in murine experimental autoimmune encephalomyelitis. *J Neurosci Res* 2010;88:3376-3385.
- 12 Davies KJ: Degradation of oxidized proteins by the 20S proteasome. *Biochimie* 2001;83:301-310.
- 13 Chondrogianni N, Stratford FL, Trougakos IP, Friguet B, Rivett AJ, Gonos ES: Central role of the proteasome in senescence and survival of human fibroblasts: induction of a senescence-like phenotype upon its inhibition and resistance to stress upon its activation. *J Biol Chem* 2003;278:28026-28037.
- 14 Zhang J, An SJ, Fu JQ, Liu P, Shao TM, Li M, Li X, Jiao Z, Chai XQ: Mixed Aqueous Extract of *Salvia Miltiorrhiza* Reduces Blood Pressure through Inhibition of Vascular Remodelling and Oxidative Stress in Spontaneously Hypertensive Rats. *Cell Physiol Biochem* 2016;40:347-360.
- 15 Zheng J, Bizzozero OA: Reduced proteasomal activity contributes to the accumulation of carbonylated proteins in chronic experimental autoimmune encephalomyelitis. *J Neurochem* 2010;115:1556-1567.
- 16 Jamart C, Gomes AV, Dewey S, Deldicque L, Raymackers JM, Francaux M: Regulation of ubiquitin-proteasome and autophagy pathways after acute LPS and epoxomicin administration in mice. *BMC Musculoskelet Disord* 2014;15:166.
- 17 Tourtellotte WG: Axon Transport and Neuropathy: Relevant Perspectives on the Etiopathogenesis of Familial Dysautonomia. *Am J Pathol* 2016;186:489-499.
- 18 Castro JP, Jung T, Grune T, Almeida H: Actin carbonylation: from cell dysfunction to organism disorder. *J Proteomics* 2013;92:171-180.
- 19 Lazarus RC, Buonora JE, Jacobowitz DM, Mueller GP: Protein carbonylation after traumatic brain injury: cell specificity, regional susceptibility, and gender differences. *Free Radic Biol Med* 2015;78:89-100.
- 20 Zhang L, Li Z, He W, Xu L, Wang J, Shi J, Sheng M: Effects of Astragaloside IV Against the TGF-beta1-Induced Epithelial-to-Mesenchymal Transition in Peritoneal Mesothelial Cells by Promoting Smad 7 Expression. *Cell Physiol Biochem* 2015;37:43-54.
- 21 Brettschneider J, Petzold A, Junker A, Tumani H: Axonal damage markers in the cerebrospinal fluid of patients with clinically isolated syndrome improve predicting conversion to definite multiple sclerosis. *Mult Scler* 2006;12:143-148.
- 22 Petzold A, Rejdak K, Plant GT: Axonal degeneration and inflammation in acute optic neuritis. *J Neurol Neurosurg Psychiatry* 2004;75:1178-1180.

- 23 Miraldi ER, Thomas PJ, Romberg L: Allosteric models for cooperative polymerization of linear polymers. *Biophys J* 2008;95:2470-2486.
- 24 Cheng G, Kong RH, Zhang LM, Zhang JN: Mitochondria in traumatic brain injury and mitochondrial-targeted multipotential therapeutic strategies. *Br J Pharmacol* 2012;167:699-719.
- 25 Tang X, Rong G, Bu Y, Zhang S, Zhang M, Zhang J, Liang X: Advanced oxidation protein products induce hypertrophy and epithelial-to-mesenchymal transition in human proximal tubular cells through induction of endoplasmic reticulum stress. *Cell Physiol Biochem* 2015;35:816-828.
- 26 Ansari MA, Roberts KN, Scheff SW: Oxidative stress and modification of synaptic proteins in hippocampus after traumatic brain injury. *Free Radic Biol Med* 2008;45:443-452.
- 27 Butterfield DA, Perluigi M, Reed T, Muharib T, Hughes CP, Robinson RA, Sultana R: Redox proteomics in selected neurodegenerative disorders: from its infancy to future applications. *Antioxid Redox Signal* 2012;17:1610-1655.
- 28 Qiusheng Z, Meng Z, Xianjian H, Xiaojia L, Weiping L: Axonal injury induced by carbonylation of cytoskeletal brain proteins in rats after traumatic brain injury. *Chin J Neuromedicine* 2015;14:469-472.
- 29 Anderson KJ, Scheff SW, Miller KM, Roberts KN, Gilmer LK, Yang C, Shaw G: The phosphorylated axonal form of the neurofilament subunit NF-H (pNF-H) as a blood biomarker of traumatic brain injury. *J Neurotrauma* 2008;25:1079-1085.
- 30 Siman R, Toraskar N, Dang A, McNeil E, McGarvey M, Plaum J, Maloney E, Grady MS: A panel of neuron-enriched proteins as markers for traumatic brain injury in humans. *J Neurotrauma* 2009;26:1867-1877.
- 31 Gyorgy A, Ling G, Wingo D, Walker J, Tong L, Parks S, Januszkiewicz A, Baumann R, Agoston DV: Time-dependent changes in serum biomarker levels after blast traumatic brain injury. *J Neurotrauma* 2011;28:1121-1126.
- 32 Gordon-Weeks PR: Microtubules and growth cone function. *J Neurobiol* 2004;58:70-83.
- 33 Dalle-Donne I, Aldini G, Carini M, Colombo R, Rossi R, Milzani A: Protein carbonylation, cellular dysfunction, and disease progression. *J Cell Mol Med* 2006;10:389-406.
- 34 Michelot A, Grassart A, Okreglak V, Costanzo M, Boone C, Drubin DG: Actin filament elongation in Arp2/3-derived networks is controlled by three distinct mechanisms. *Dev Cell* 2013;24:182-195.
- 35 Normoyle KP, Briehier WM: Cyclase-associated protein (CAP) acts directly on F-actin to accelerate cofilin-mediated actin severing across the range of physiological pH. *J Biol Chem* 2012;287:35722-35732.
- 36 Zheng J, Bizzozero OA: Reduced proteasomal activity contributes to the accumulation of carbonylated proteins in chronic experimental autoimmune encephalomyelitis. *J Neurochem* 2010;115:1556-1567.
- 37 Pickering AM, Koop AL, Teoh CY, Ermak G, Grune T, Davies KJ: The immunoproteasome, the 20S proteasome and the PA28alpha proteasome regulator are oxidative-stress-adaptive proteolytic complexes. *Biochem J* 2010;432:585-594.
- 38 Bulteau AL, Lundberg KC, Humphries KM, Sadek HA, Szweda PA, Friguet B, Szweda LI: Oxidative modification and inactivation of the proteasome during coronary occlusion/reperfusion. *J Biol Chem* 2001;276:30057-30063.
- 39 Bulteau AL, Verbeke P, Petropoulos I, Chaffotte AF, Friguet B: Proteasome inhibition in glyoxal-treated fibroblasts and resistance of glycated glucose-6-phosphate dehydrogenase to 20 S proteasome degradation *in vitro*. *J Biol Chem* 2001;276:45662-45668.
- 40 Farout L, Mary J, Vinh J, Szweda LI, Friguet B: Inactivation of the proteasome by 4-hydroxy-2-nonenal is site specific and dependant on 20S proteasome subtypes. *Arch Biochem Biophys* 2006;453:135-142.